European Journal of Neuroscience, Vol. 20, pp. 1391–1401, 2004

Directed interactions between visual areas and their role in processing image structure and expectancy

Rodrigo F. Salazar,[1] Peter König[1,2] and Christoph Kayser[1,*]
[1]Institute of Neuroinformatics, University & ETH Zürich, Winterthurerstrasse 190, 8057 Zürich, Switzerland
[2]Institute for Cognitive Science, University Osnabrück, Albrechtstr. 28, 49069 Osnabrück, Germany

Keywords: cat, gamma oscillations, Granger causality, local field potential, multivariate analysis

Abstract

During sensory processing, cortical areas continuously exchange information in different directions along the hierarchy. The functional role of such interactions, however, has been the subject of various proposals. Here, we investigate the role of bottom-up and top-down interactions in processing stimulus structure and their relation to expected events. Applying multivariate autoregressive methods to local field potentials recorded in alert cats, we quantify directed interactions between primary (A17/18) and higher (A21) visual areas. A trial-by-trial analysis yields the following findings. To assess the role of interareal interactions in processing stimulus structure, we recorded in naïve animals during stimulation with natural movies and pink noise stimuli. The overall interactions decrease compared with baseline for both stimuli. To investigate whether forthcoming events modulate interactions, we recorded in trained animals viewing two stimuli, one of which had been associated with a reward. Several results support such modulations. First, the interactions increase compared with baseline and this increase is not observed in a context where food was not delivered. Second, these stimuli have a differential effect on top-down and bottom-up components. This difference is emphasized during the stimulus presentation and is maximal shortly before the possible reward. Furthermore, a spectral decomposition of the interactions shows that this asymmetry is most dominant in the gamma frequency range. Concluding, these results support the notion that interareal interactions are more related to an expectancy state rather than to processing of stimulus structure.

Introduction

Sensory stimuli are processed across many cortical areas joined by a network of complex connectivity (Felleman & Van Essen, 1991; Van Essen *et al*., 1992). By the virtue of this connectivity, sensory areas continuously exchange information along the two hierarchical directions: bottom-up and top-down. Concerning bottom-up signals, the general consensus is that they reflect the physical properties of the stimulus and relay this information to higher areas. In contrast, the role of top-down signals is the subject of various proposals.

In the visual system, top-down signals have been suggested to modulate activity in lower areas according to the global structure of the stimulus. Thus, they should play an important role in perceptual grouping and figure-ground segmentation. Support for this hypothesis comes from experiments in which inactivation of higher areas decreased the sensitivity of cells to stimuli of low salience (Hupe *et al*., 1998; Bullier *et al*., 2001), altered their tuning properties (Wang *et al*., 2000; Galuske *et al*., 2002) and abolished figure-ground segmentation (Lomber *et al*., 1994). Correlates of figure-ground segmentation were found in the responses of single neurons. Whether the receptive field of a neuron lies within the same texture as part of the figure or as part of the background affects neuronal responses. However, this effect occurs only with a delay, which supposedly reflects top-down influences (Lamme *et al*., 1998; Lamme & Roelfsema, 2000).

Another line of research focuses on the relationship between interareal interactions and the predictive power of behavioural contexts (see Engel *et al*., 2001 for a review). These studies emphasize the role of top-down signals in transmitting predictions generated by higher areas to lower processing stages. As a consequence, expectations should be manifested in sensory areas. Evidence comes from experiments where expected stimuli induce synchronization between local field potentials at different hierarchical levels (Roelfsema *et al*., 1997). A phase analysis of local field potentials suggests that this effect is attributable to top-down signals (von Stein *et al*., 2000).

Here, we evaluate the role of directed interareal interactions in processing stimulus structure and their relation to expected events. We recorded local field potentials in the primary visual cortex (A17/18) and the higher visual area A21a of alert cats. We use multivariate autoregressive (MVAR) modelling of the data to quantify the directed interactions between these areas. First, in trained animals, we compare interactions during passive viewing of two gratings, one of which predicts a forthcoming food delivery. If top-down signals carry information about expected events, they should dominate the interactions for the stimulus associated with the food compared with the other stimulus. Then we compare the strength of interactions in naïve animals during stimulation with natural movies and a derived pink noise stimulus. If top-down signals are related to the stimulus structure, they should dominate the interactions upon stimulation with natural movies compared with the noise.

Correspondence: Dr R.F. Salazar, as above.
E-mail: salazar@ini.phys.ethz.ch
**Present address*: Max Planck Institute for Biological Cybernetics, Spemannstrasse 38, 72076 Tübingen, Germany

Received 26 February 2004, revised 17 June 2004, accepted 25 June 2004

doi:10.1111/j.1460-9568.2004.03579.x

Materials and methods

Subjects and recording technique

Data were obtained from four female cats. Two of them were trained to recognize two orthogonal sine-wave gratings, referred to as S+ and S–. The animals had to indicate the presence of S+ by pressing a lever in order to receive a food reward (for details about the training procedure, see Salazar *et al*., 2004). The other two animals are referred to as naïve animals. The raw data of the experiments presented below have already been used for different analyses in two previous studies (Kayser *et al*., 2003; Salazar *et al*., 2004).

In each subject, a small microdrive featuring four movable electrode bundles was implanted under sterile conditions using halothane/N_2O anaesthesia (1–1.5% and 70%, respectively; for details, see Kayser *et al*., 2003). Two bundles were placed over the primary visual areas A17/18 and two over the visual area A21a. The two bundles within the same area were spaced 1–2 mm apart laterally. Each bundle consisted of four electrode wires twisted closely together (< 50 μm apart). The local field potential on each of these four electrodes was very similar. The average within-bundle correlation was 0.82, whereas the cross-bundle correlation was only 0.27. Therefore, we averaged the signals of the four electrodes of each bundle to obtain one local field potential from the respective recording site. The depth of each electrode bundle was changed regularly, usually every couple of days. Overall, we obtained data from 23 different groups of recording sites (each group = 4 sites) in the trained animals and 15 different groups of sites in the naïve animals. The correct positioning of the electrodes in the respective anatomical areas was verified later using standard histological procedures (anaesthesia with ketamine/xylazine and overdose of pentobarbital intravenously; heart perfusion with saline and then paraformaldehyde; cortical slices stained with Nissl). For each recording site and stimulus, we recorded between 45 and 180 repeats of the stimulus.

Recording procedures and stimulation protocol

For recordings, the animals were first restrained by a sleeve equipped with adjustable Velcro fasteners and then placed in an acrylic tube allowing stable positioning in front of the monitor. The animal's head was fixed using screws inserted into the chronic implants. During the experiment, the state of alertness of the animal was assessed with an infrared camera system and by examining the local field potential online. Based on these controls, the animals seemed to be alert and were not drowsy or sleeping. All procedures were in accordance with the Zürich cantonal guidelines for the use of experimental animals and conformed to the American National Institutes of Health and Society for Neuroscience regulations.

During recording, the animals passively viewed different stimulus paradigms.

Grating–food

The trained cats viewed presentations of the two orthogonal drifting sine-wave gratings that they previously learned to recognize in a go/no go paradigm (spatial frequency 0.16 cycles/°, temporal frequency 1.6 cycles/s). One of them, referred to as S+, was associated with a food reward upon correct response. The other grating, referred to as S–, was never rewarded. To maintain the association of S+ with food reward during passive viewing, drops of liquefied cat food were delivered after stimulus offset (see Salazar *et al*., 2004 for details).

Movie–noise

Both the trained and the naïve animals viewed two types of stimuli differing in their global structure. The first type consisted of three natural movies. These movies were recorded from a camera placed on the head of a freely moving cat in a natural environment (Betsch *et al*., 2004). The second type was a modified version of the natural movies in which the higher order structure was randomized. This stimulus is known as pink noise and has the same spatio-temporal power spectrum as the original movie (see Kayser *et al*., 2003 for details).

Grating

Both the trained and the naïve animals viewed sine-wave gratings of the same spatial and temporal frequency and orientation as S+ and S–. In contrast to the grating–food set, these stimuli were shown in a different context. They were randomly mixed with other gratings of different orientation and no food was delivered.

In all paradigms, stimuli were shown in a random order and separated by a uniform grey screen (blank). All stimuli had the same mean luminance as the blank and same root mean squared (r.m.s.) contrast. Stimuli were presented on a 19′ Hitachi CRT monitor (120 Hz refresh rate) placed 0.5 m in front of the animal in a darkened room. The stimuli were presented using MATLAB (Mathworks, Natick, USA) code based on the psychophysics toolbox extensions (Brainard, 1997; Pelli, 1997).

Signal processing and data analysis

Signals picked up by the electrodes were first passed through a 24-channel preamplifier (Neurotrack, 10-fold amplification), then amplified and digitized using a Synamps system (Neuroscan, El Paso, USA) at a temporal resolution of 20 kHz using a high-pass filter of 5 Hz. Off-line analysis of the local field potentials was carried out in MATLAB. The local field potential was extracted by band-pass filtering the data between 5 and 125 Hz and resampling at 250 Hz.

The analysis of the interactions was based on a MVAR modelling of the local field potential time series. From these MVAR models, a measure of directed interactions, the Wiener–Granger causality and its spectral decomposition were extracted. Details of these methods have been described in the literature in detail (Bernasconi & König, 1999; Ding *et al*., 2000). It was previously shown that these measures of interactions can be effectively applied to local field potential recordings from *in vivo* preparations and awake animals (Bernasconi & König, 1999; Freiwald *et al*., 1999; Ding *et al*., 2000; Liang *et al*., 2000; Baccala & Sameshima, 2001; Kaminski *et al*., 2001; Liang *et al*., 2002).

MVAR model

Let X_t denote the vector describing the two channels from area A17/18 and let Y_t be the vector containing the two channels from area A21a. Let Z denote the vector containing the data from all four channels, i.e. $Z = [X, Y]$. The MVAR model expresses the values at time t as a weighted sum of the past values and thus describes a linear prediction of future data based on past values (Fig. 1). There are three models. Two of them describe the channels of the two areas based on their own data and one model expresses the data of each channel based on the data from all four channels:

$$\begin{aligned} X_t &= c_x + A_{1,x}X_{t-1} + \ldots + A_{p,x}X_{t-p} + \varepsilon_{t,x} \\ Y_t &= c_y + A_{1,y}Y_{t-1} + \ldots + A_{p,y}Y_{t-p} + \varepsilon_{t,y} \\ Z_t &= c_z + A_{1,z}Z_{t-1} + \ldots + A_{p,z}Z_{t-p} + \varepsilon_{t,z} \end{aligned} \quad (1)$$

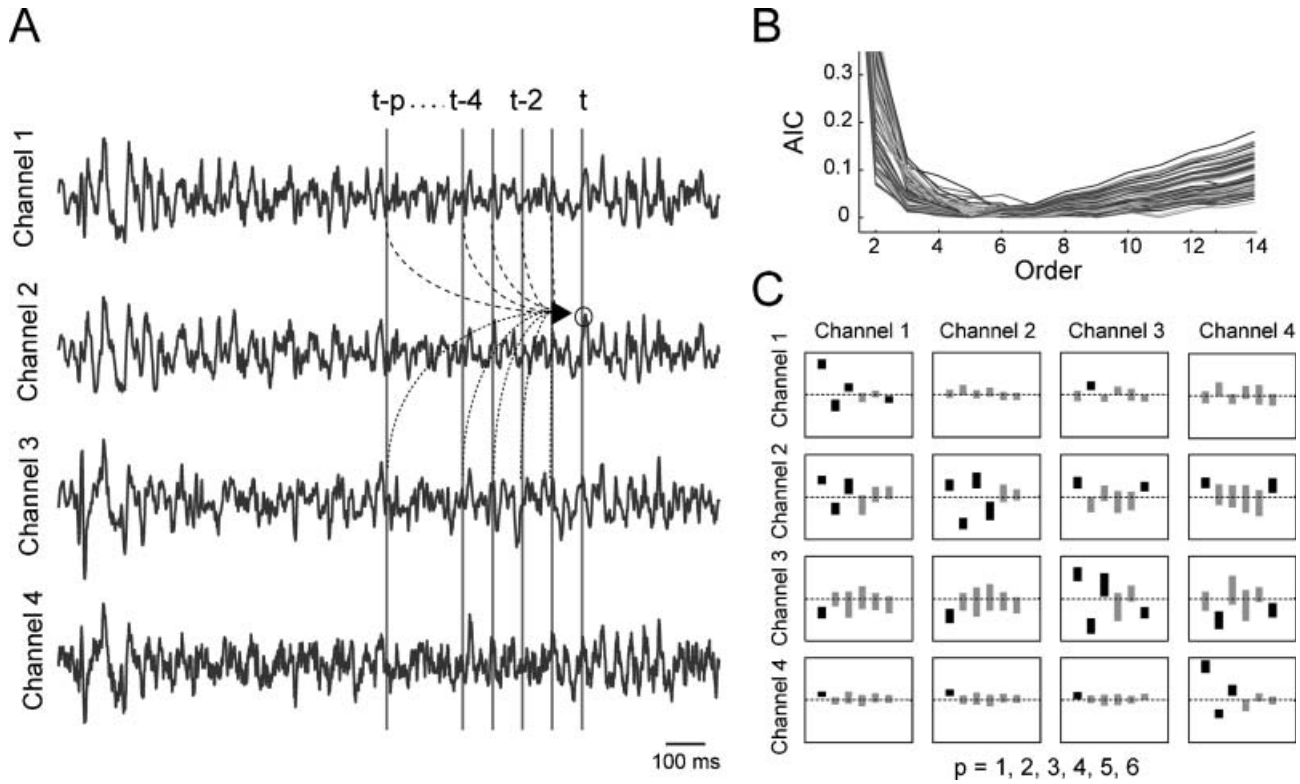

FIG. 1. Example data and autoregressive modelling. (A) Local field potentials recorded at four sites during the presentation of a stimulus. The MVAR model expresses the data of one site at time point t (small circle, Chan 2) using a linear combination of the data from all channels at the past time points t, $t-1$, …, $t-p$, where p represents the order of the MVAR model. (B) The graph shows the AIC for several recording sites. The AIC is used to choose the optimal model order and characterizes the balance between a minimal p and a good fit to the data. The local minimum represents the optimal choice and is between 5 and 7. (C) The coefficients of the MVAR model for one group of recording sites during the movie–noise condition. The model order was 6 and thus there are 6 coefficients for each pair of channels. The boxes represent the distribution of coefficients (mean ± SD) obtained for 60 repeats of the stimulus. Black boxes represent coefficients for which the mean is significantly different from zero (t-test, $P < 0.05$), grey boxes represent insignificance.

Here c are constants, p is the order of the model, the matrices A_i contain the model coefficients and ε_t are the residuals, which are white noise processes. Thus, $E[\varepsilon_{t,x}] = 0$ and $E[\varepsilon_{t,x}\ \varepsilon_{\tau,x}{}']$ is non-zero only if $t = \tau$; similarly for y and z.

$$\begin{aligned} E[\varepsilon_{t,x}\varepsilon_{t,x}{}'] &= \Omega_{17/18}, \\ E[\varepsilon_{t,y}\varepsilon_{t,y}{}'] &= \Omega_{21} \text{ and} \\ E[\varepsilon_{t,z}\varepsilon_{t,z}{}'] &= \tilde{\Omega}_{\text{all}} \end{aligned} \tag{2}$$

Because Z consists of X and Y, the latter can be decomposed into:

$$\tilde{\Omega}_{\text{all}} = \begin{pmatrix} \tilde{\Omega}_{17/18} & C \\ C & \tilde{\Omega}_{21} \end{pmatrix}$$

with C being the cross-area covariance matrix. The matrices Ω are the important characteristics for the computation of the causality measures (see below). The models for X and Y can be obtained as a subset of the model for Z, and in the following we will concentrate on the latter when describing the quality of the fitted models.

The model coefficients are chosen such that the model optimally reproduces the original data in the mean square sense. Here the coefficients were obtained using the Levinson, Wiggins, Robinson algorithm (Haykin & Kesler, 1983).

The order of the model p needs to be specified in advance and requires a compromise between a good fit to the data and a good prediction of future data. A widely used criterion is based on the Akaike Information Criterion (AIC; Akaike, 1974; Bernasconi & König, 1999):

$$\text{AIC}(p) = \log(\det(\Omega)) + 2n_{\text{est}}/T$$

where Ω is the estimated noise covariance, n_{est} is the total number of free parameters ($4*4*p$) and T is the length of the data window used to estimate the model. The first term decreases with increasing p, while the second term punishes models with a high order. We tested all values of p between 4 and 14 on our entire set of data. Example values of AIC are shown in Fig. 1B for one typical recording session. These curves have a minimum between $p = 5$ and 7. As a compromise, we choose the order of the model to be $p = 6$.

There are two ways in which the model can be determined for a given dataset. In a first approach, the model is fitted to the data of each trial separately and the causality measures are computed for each trial. Then, only these measures are averaged across trials to yield one result for a given group of recording sites. This conservative approach regards different trials as potentially different processes and reduces the variance only in the last step when averaging the causality measures across trials. In a second approach (Ding *et al.*, 2000) the data of different trials are taken as realizations of the same underlying stochastic process. To compute the model coefficients, the different trials are first combined and only one set of MVAR coefficients is obtained for this dataset. This approach has the advantage that the variance is reduced before fitting the MVAR model, which is the non-linear step in the analysis. In the following, we will refer to the first

approach as 'trial-by-trial' analysis and to the second as 'ensemble' analysis. For the main part of the analysis, we focus on the trial-by-trial approach and use the ensemble approach as a control.

For both approaches, the MVAR models were estimated separately for several windows (800 ms long): one during the blank screen (800 ms prior to and until stimulus onset); one window shortly after stimulus onset but excluding the initial evoked response (200–1000 ms after stimulus onset); a second stimulus window (1200–2000 ms after stimulus onset). For the grating–food paradigm, which lasted 3000 ms, a third stimulus window (2200 and 3000 ms after stimulus onset) was used in some specified cases.

Prerequisites and quality of the fitted MVAR models

In order for the MVAR description of the experimental data to be valid, several conditions must be satisfied. First, the data must have a Gaussian distribution. This was verified by computing the histogram of the data for each trial, window and electrode. The histogram was then compared with a normal distribution of the same variance using a Kolmogorov–Smirnov test (see Fig. 2a for examples). In more than 98% of the cases the data did indeed follow a Gaussian distribution (based on a *P*-value of 0.01, no correction for multiple testing).

A second important prerequisite for the MVAR modelling is that the data must be stationary. To test this, each data window was split into half and the data from the first half were compared with the data from the second half. Stationary was assumed if these two distributions did not differ significantly (Kolmogorov–Smirnov test, $P > 0.05$, no correction for multiple test). A previous study showed the reliability of this procedure (Bernasconi & König, 1999). Two example trials are shown in Fig. 2B. The left part shows the local field potentials from the four recording sites. The right part shows the two histograms used for stationary testing for the data of one of these channels. In the upper trial, the data are stationary while in the lower trial the data are not. In the latter case, the signal amplitude increases during the second half. For each window, the data were accepted as stationary if the signals at all four recording sites were stationary. Overall, 85% of the windows were accepted as stationary. Figure 2B shows the distribution of stationary trials across the different stimulation conditions. Interestingly, during the presentation of a stimulus the data were more likely to be stationary (88.1% of the windows) than during the blank (78.2% of the windows), and this difference was significant (*t*-test, $P < 0.01$). In contrast, the different stimuli did not differ significantly in the percentage of stationary trials ($P > 0.05$ for all pairwise comparisons).

If the MVAR model correctly describes the data and thus incorporates all the temporal structure, the residual ε_t [cf. Eq. (1)] will describe a white noise process. We verified this in the following way (see Ding *et al*., 2000 for more details). For each residual, all auto- and cross-correlations were computed up to lag 6. We then tested the null hypothesis that the residual had no correlations and, thus, all correlation coefficients should be within a 5% significance interval around zero based on a *t*-statistic. For each trial and window, we counted the number of correlation coefficients that were outside of this interval. In all cases, less than 3% of the correlation coefficients were significantly different from zero.

In a second step, we quantified what proportion of the correlation structure of the original data was actually captured by the MVAR models (see Ding *et al*., 2000 for more details). To do so, for each fitted MVAR model, an artificial dataset was created by iterating the model on the initial values of the experimental data. Then, all auto- and cross-correlations were computed for both the artificial and experimental datasets. The two vectors defined by all correlation coefficients (R_{real} and R_{artif}, respectively) were then compared to yield the following consistency measure:

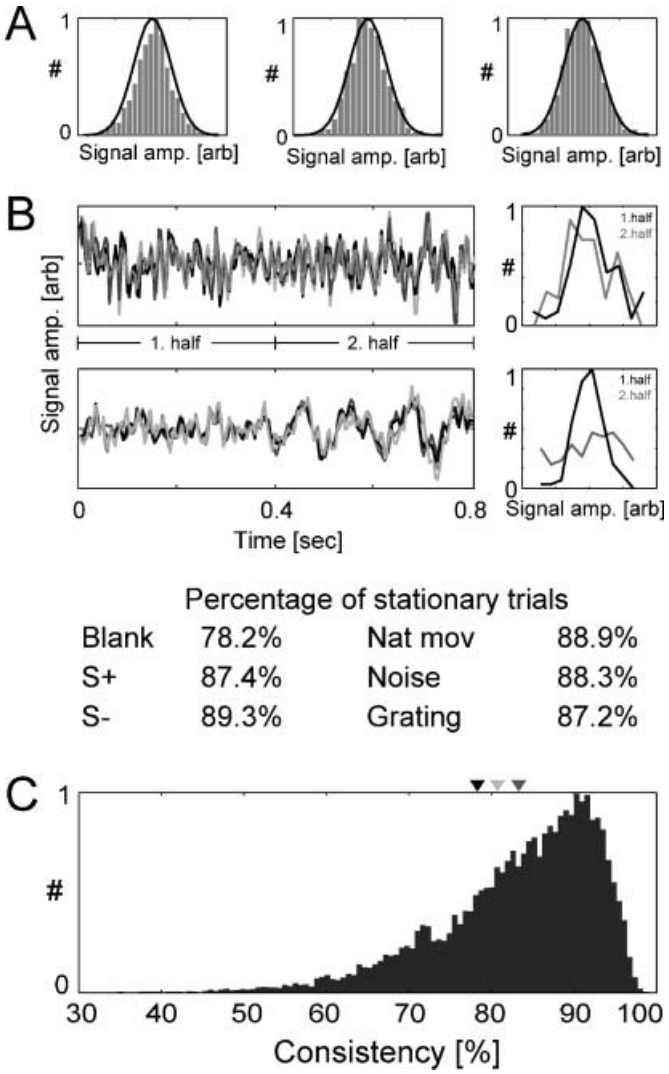

FIG. 2. Prerequisites for a successful MVAR modelling of the neuronal data. (A) Testing for Gaussian distribution of the data. For three windows the histograms of the data are shown together with a fitted Gaussian distribution of the same mean and variance (solid line). In all cases, these two distributions do not differ significantly (*t*-test, $P > 0.05$). (B) Testing for stationarity of the data in two example trials (upper and lower panels). On the left, the data from the four recording sites are shown (different grey scales for different channels). On the right, the histograms of the data during the first and the second half are shown, always for one of the four channels. In the upper example the data are stationary. The two histograms from the first and second half do not differ significantly (Kolmogorov–Smirnov test, $P > 0.05$). In the lower example the data are not stationary: the amplitudes increase during the second half. The two histograms differ significantly and this was the case for all four channels ($P < 0.05$). (C) Consistency of the temporal structure in the original data and in the MVAR model. The percent consistency measure (*PC*) indicates how well the temporal structure of experimental and modelled data matched. The graph shows the histogram of the *PC* values for all trials and data windows. The overall mean was 83%. The different paradigms differ slightly in their mean consistency (triangles on top): 78.4% for the grating–food (black triangle); 83.3% for the movie–noise (dark grey) paradigms, respectively; and 81.1% during the blank (light grey).

$$PC = \left(1 - \frac{|R_{\text{real}} - R_{\text{artif}}|}{|R_{\text{real}}|}\right) \times 100 \quad (3)$$

Here, |…| denotes the 1-norm (sum of absolute values of all vector elements). Figure 2C shows the distribution of the consistency measure for all data windows including blank and stimulus. On average the consistency was 83%, which is close to values reported in another study (Ding *et al*., 2000). Models fitted to the trials of the grating–food paradigm showed a slightly lower consistency than those of the movie–noise paradigm (78.4% vs. 83.3%). These numbers were not significantly different ($P > 0.05$) from the consistency obtained during the blank (81.1%). Concluding, we can confidently say that the MVAR models captured the temporal structure of the experimental data.

As a last control, we computed the average r.m.s. error between the experimental data and those predicted using the model. On average, this r.m.s. error was only 4.75% of the standard deviation of the respective signal. However, for a few trials the model gave an inaccurate description of the data and the error was large. As a good description of the raw data is crucial for the validity of the measured interactions, we employed the following criterion to detect these trials. We computed the distribution of all r.m.s. errors. The trials, for which the r.m.s. error was more then two standard deviations above the mean of this distribution, were denoted as 'large error trials'.

We performed the entire analysis of the interactions twice. First, we just used trials that were stationary and did not belong to the 'large error trials'. These two criterions together lead to an exclusion of 32% of the data windows (24% for the grating–food and 34% for the movie–noise paradigm, respectively). Second, we used all the trials. In this case, some of the trials do not fulfil the criteria necessary for a valid description by a MVAR model. The purpose of this second analysis was to check whether the selection of trials affects the main results. However, this is not the case and the results of both analyses were qualitatively the same (see the Results for details).

Causality measures

The direction of information flow between the recorded channels was studied using structural analysis of the time series. Two methods to quantify the interactions were used: the Wiener–Granger causality measure and the directed transfer function. The Wiener–Granger measure of causality (Granger, 1963, 1969, 1980) is based on the intuitive idea that if a time series X causes the time series Y, the knowledge of the past of X and Y should improve predictions of the present value of Y, compared with knowledge of the past of Y alone. For multivariate stationary processes, Geweke proposed a measure of linear dependence (information) between two groups of variables that can be obtained form the MVAR coefficients (Geweke, 1982). Define $\text{var}(X|Y)$ as the mean square error of the prediction of the best linear forecast of a time series X based on the knowledge of Y. Let X^- be the past and X^+ the past and present of X, and let X indicate the whole time series. Then the following represents a measure of linear dependence between the time series X and Y:

$$\begin{aligned} F_{X,Y} &= \log\left\{\frac{\det[\text{var}(X/X^-)]}{\det[\text{var}(X/X^-, Y)]}\right\} \\ &= \log\left\{\frac{\det[\text{var}(Y/Y^-)]}{\det[\text{var}(Y/Y^-, X)]}\right\} \end{aligned} \quad (4)$$

Here, det denotes the determinant of the matrix. This quantity can be decomposed into directional measures of linear interactions, $F_{X\to Y}$ and $F_{Y\to X}$, and into an instantaneous interaction F_{inst}: $F_{X,Y} = F_{X\to Y} + F_{Y\to X} + F_{\text{inst}}$. Here, $F_{X\to Y}$ can be interpreted as a number quantifying how much the generalized variance of the prediction error of Y is reduced, when Y is predicted not only based on itself alone but also based on X. Furthermore, these measures can be expressed in the frequency domain (for details, see Bernasconi & König, 1999). Given the MVAR model of the data, these interaction measures can be obtained from the error variance matrices in Eq. (2):

$$\begin{aligned} F_{17/18\to 21a} &= \log(\det(\Omega_{21a}/\det(\tilde{\Omega}_{21a})) \\ F_{21a\to 17/18} &= \log(\det(\Omega_{17/18}/\det(\tilde{\Omega}_{17/18})) \\ F_{\text{inst}} &= \log(\det(\tilde{\Omega}_{17/18})^*\det(\tilde{\Omega}_{21a})/\det(\Omega_{\text{all}})) \end{aligned} \quad (5)$$

The instantaneous interaction F_{inst} reflects either a flow of information too fast to be detected by the sampling rate used, or common inputs to the time series. However, as can be seen from the formula, it does not carry any directed information. Thus, in the following, we focus on the two directional measures. $F_{17/18\to 21a}$ and $F_{21a\to 17/18}$ reflect the bottom-up and top-down components of the signal, respectively, and will be referred to as such. To investigate the relative changes of interareal interactions induced by the stimulus, we computed the percent change of the information flow with respect to the blank. We define the modulation of the top-down (*TD*) and bottom-up (*BU*) components as the following:

$$BU = 100 \times \frac{F^{\text{Stimulus}}_{17/18\to 21a} - F^{\text{Blank}}_{17/18\to 21a}}{F^{\text{Blank}}_{17/18\to 21a}} \quad (6)$$

$$TD = 100 \times \frac{F^{\text{Stimulus}}_{21a\to 17/18} - F^{\text{Blank}}_{A21a\to 17/18}}{F^{\text{Blank}}_{21a\to 17/18}} \quad (7)$$

The following analysis concentrates on these two quantities. These quantities were averaged across all stimulus repeats for a given group of recording sites yielding one number for top-down and bottom-up, respectively. For statistics, these numbers were averaged across groups of recording sites and the significance level was assessed using *t*-tests.

As a second measure of interactions, we employed the concept of the directed transfer function (Jenkins & Watts, 1968; Ding *et al*., 2000). The directed transfer function is obtained from a spectral decomposition of the MVAR model and is closely related to the Wiener–Granger interaction measure (see Baccala & Sameshima, 2001 for details).

Results

Effect of expectations

To quantify the overall modulation of the interareal interactions by the different stimuli, we first investigate the total interactions: the sum of the bottom-up and top-down components (Fig. 3, left). This total interaction was averaged across the two windows during the stimulus presentation. For both stimuli of the grating–food paradigm, the total interaction increases during the stimulus presentation. Both increases are significant (S^+: stimulus associated with food, $P < 0.0001$; S^-: stimulus not associated with food, $P < 0.05$). Furthermore, this effect is specific to a situation where forthcoming events are predictable. When the same stimuli were shown interleaved with other stimuli and without food deliveries, as in the grating paradigm, the total interaction is not affected ($P > 0.05$).

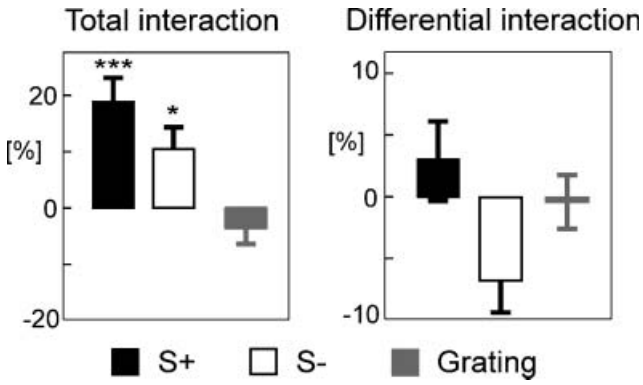

FIG. 3. Interactions during the grating–food and grating paradigms (trained animals). Left panel: total interaction defined as the sum of top-down and bottom-up interactions (*TD* + *BU*) and normalized as percent change compared with the preceding blank. Right panel: differential interaction defined as the difference of top-down and bottom-up (*TD* − *BU*). The data were averaged across the two stimulus windows. The bars and the error bars represent the mean across groups of recording sites and the SEM, respectively. Significant differences from zero are marked with asterisks at $*P < 0.05$ and $***P < 0.001$.

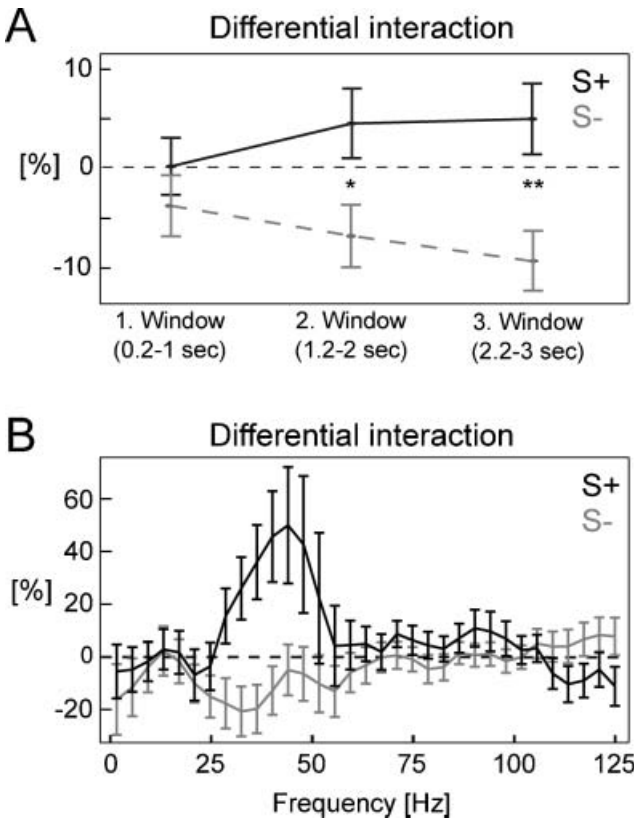

FIG. 4. Temporal development and frequency decomposition of the differential interaction in the grating–food paradigm. (A) The differential interaction analysed in the different windows separately. The time intervals indicated are referenced to the stimulus onset. (B) Frequency analysis of the differential interaction during the last window (2.2–3 s after stimulus onset). In both panels, means are computed across groups of recording sites and error bars denote the SEM. Significant differences between stimuli are marked with asterisks at $*P < 0.05$, $**P < 0.01$.

To characterize the role of bottom-up and top-down components, we investigate the differential interaction defined by the difference between top-down and bottom-up (*TD* − *BU*). As before, the data were averaged across the two windows during the stimulus presentation (Fig. 3, right). We find that the two stimuli of the grating–food paradigm emphasize different components of the interactions. The stimulus S^+ leads to a dominance of top-down interactions, whereas the other stimulus S^- leads to a dominance of bottom-up. This difference between the two stimuli is close to significance ($P = 0.08$). On the other hand, in the grating paradigm, both the top-down and bottom-up components are similar ($P > 0.05$).

To further investigate the dynamics of bottom-up and top-down interactions in the grating–food paradigm, we analyse each window separately (Fig. 4A). Interestingly, the difference between the two stimuli is more and more pronounced towards the end of the stimulus presentation, that is, in proximity to a possible delivery of food. More precisely, during the first window, bottom-up and top-down interactions are in balance for both stimuli ($P > 0.05$). In the second window, the differential interactions are dominated by top-down signals (positive value) during S^+ and by bottom-up signals during S^- (negative value). The difference between stimuli is significant ($P < 0.05$). In the third window, this latter effect is even more pronounced ($P < 0.01$), although a significant difference from zero is only reached for S^- ($P < 0.05$) and not for S^+ ($P > 0.05$). Thus, the relation between top-down and bottom-up signals is dynamic and depends on the proximity of expected events.

The results presented above indicate that bottom-up and top-down signals are differently related to expected events. To further characterize this asymmetry and localize it within the signal's spectrum, we compute a frequency decomposition of the Wiener–Granger causality measure. The difference between normalized top-down and bottom-up interactions is computed in each window separately. In the first window, no evident difference is observed between the stimuli S^+ and S^-. In accordance with the above results, in the second stimulus window, the stimulus S^+ is dominated by top-down interactions and the stimulus S^- is dominated by bottom-up interactions. This difference is even more prominent in the last window, which is displayed in Fig. 4B. This figure shows that the difference between the two stimuli is most pronounced between 20 and 60 Hz. Thus, the effect of expectancy is most prominent in the gamma frequency range.

Effect of stimulus structure

The movie–noise paradigm is analysed separately for the trained (Fig. 5, upper panel) and the naïve animals (Fig. 5, lower panel). Nevertheless, both groups of animals yield similar results. The total interaction decreases for both stimuli significantly ($P < 0.01$ and $P < 0.05$ for movie and noise in the trained animals, and $P < 0.001$ for both stimuli in the naïve animals; Fig. 5, left). This effect is specific to complex stimuli such as natural movies and pink noise but not to simpler stimuli such as gratings. In the grating paradigm, the total interaction is not different from zero ($P > 0.05$) in trained as well as in naïve animals. Thus, the spatial complexity of a stimulus affects the flow of information between areas.

The differential interactions during the movie–noise paradigm show a general tendency for a dominance of top-down interactions. Indeed, the differential interactions are positive in both the trained and naïve animals. However, none of these interactions is significantly different from zero and thus is similar to the differential interactions induced in the grating paradigm ($P > 0.05$ in all cases). Furthermore, the differences between natural movies and the pink noise are much

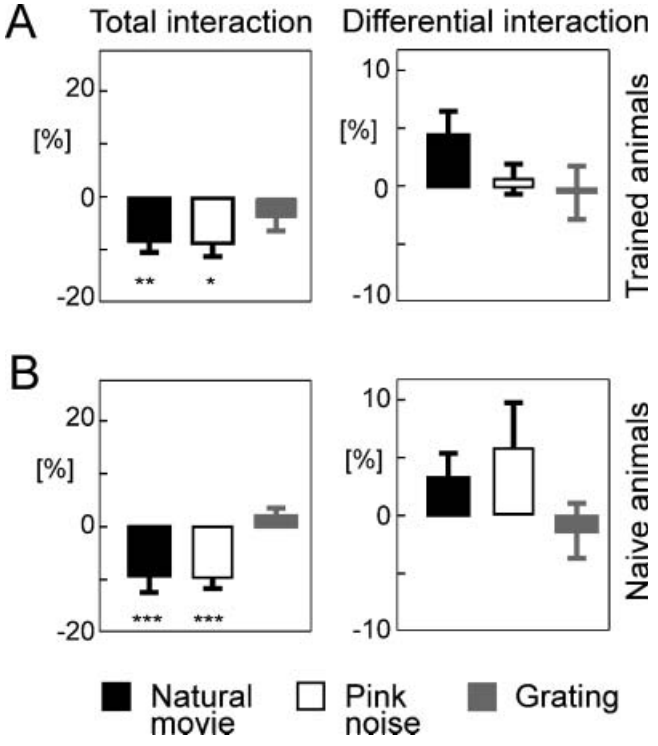

FIG. 5. Interactions in the movie–noise and grating paradigms for the trained animals (A) and naïve animals (B). Left panel: total interaction. Right panel: differential interaction. As in all figures the mean was computed across groups of recording sites and error bars denote the SEM. Significant differences from zero are marked with asterisks at $*P < 0.05$, $**P < 0.01$ and $***P < 0.001$.

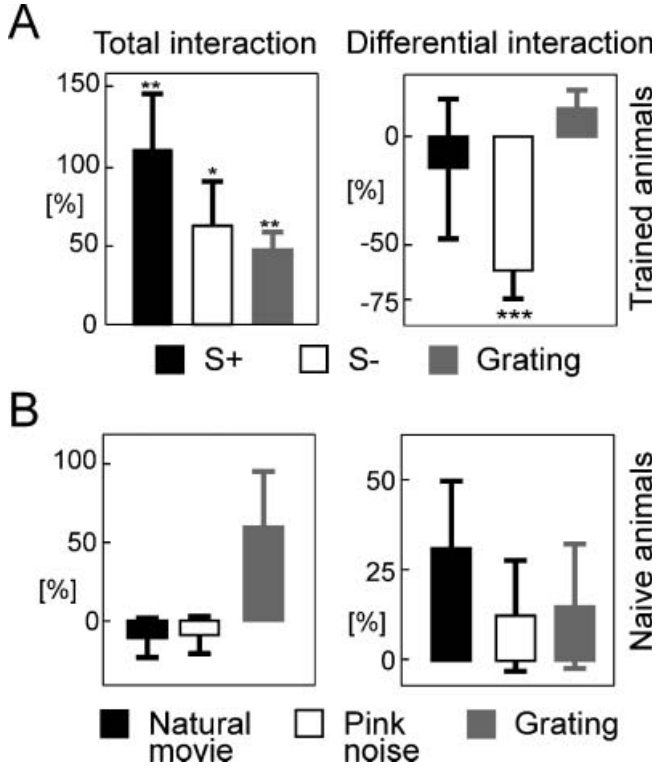

FIG. 6. Control analysis in which the MVAR model was computed using the ensemble approach. (A) The results for the trained animals in the grating–food and grating paradigms. Note that this figure should be compared with Fig. 3. (B) The results for the naïve animals in the movie–noise and grating paradigms. Note that this figure should be compared with Fig. 5B. The mean was computed across groups of recording sites and error bars denote the SEM. Significant differences from zero are marked with asterisks at $*P < 0.05$, $**P < 0.01$ and $***P < 0.001$.

smaller than the difference between S^+ and S^- as reported above for the grating–food paradigm.

To further investigate the temporal dynamics of interareal interactions, we analyse the different windows separately. In the naïve animals, there is no difference between movie and noise in any of the windows ($P > 0.05$). In the trained animals, the difference between movie and noise reaches significance only in the second window ($P < 0.05$) but not the first one ($P > 0.05$). This difference is due to a dominance of top-down interactions for natural movies (data not shown). Nevertheless, the difference between movie and pink noise (7.25%) is still smaller than the difference between S^+ and S^- (11.36%) in the same window. Summarizing, the stimulus structure has only a weak effect on interareal interactions compared with those induced by stimuli in the grating–food paradigm. Furthermore, the relative strength of bottom-up and top-down interactions does not show a tendency that is consistent between both groups of animals.

Methodological controls

The above results were obtained by neglecting trials during which the data were not stationary or for which the fitted MVAR model did not reproduce the original data well. We performed an additional analysis, but this time included all available data, even if the trial did not fulfil the prerequisites of the MVAR modelling. Although the results obtained differ numerically from those presented above, they are qualitatively the same. To test this more rigorously, for each of the quantities shown in Figs 3 and 5 we performed a pair-wise comparison between the results obtained using either all or only the restricted set of trials. In all cases, the two analyses yield similar results (*t*-test, $P > 0.05$). Therefore, we can rule out the possibility that the results presented above are biased by the selection of the trials.

There are two approaches, based on different assumptions, to compute the MVAR models for a given set of trials (see Materials and methods). One approach is to compute the model for each trial separately and then average the interaction measures across trials ('trial-by-trial' analysis). As the model is computed for each trial separately, this approach does not assume any similarity across trials of the underlying multivariate model describing the interactions. In principle, the pattern of the interactions could differ completely in each trial and the results obtained represent only the average effect. This approach was used to obtain the results presented above. A second approach is to assume that all trials for a given stimulus are realizations of the same stochastic process and that fluctuations from trial to trial are small deviations from a fixed model. To estimate this model, the different trials are combined before fitting the MVAR model ('ensemble analysis'). On one hand, the variance is reduced before the non-linear fitting process resulting in a better signal to noise ratio. On the other hand, the ensemble analysis makes the additional assumption of stationarity over all trials.

For a comparison of the two approaches, we perform the ensemble analysis on the same dataset, again excluding trials, which shows no stationarity already within the trial (Fig. 6). Overall we find that the results differ quantitatively from the trial-by-trial analysis. The stimulus-induced changes of the interactions are much larger (roughly by a factor of 5) than the results obtained from the trial-by-trial

analysis. This indicates a greater sensitivity of the ensemble analysis to stimulus-induced interactions. In the following, we will show that despite these quantitative changes some of the main findings are preserved, especially in the grating–food paradigm. However, the significance of other findings, mainly in the movie–noise and grating paradigms, is altered. More precisely, for the trained animals, both stimuli of the grating–food paradigm lead to a significant increase of the total interactions (Fig. 6A, left). In the ensemble analysis, however, the dominance of bottom-up components for S^- is significant already when averaged across all windows ($P < 0.001$; Fig. 6A, right). In the grating paradigm, the trial-by-trial analysis did not reveal any significant effect of the stimulus on the interactions. In contrast, the ensemble analysis yields a significant increase of the interactions ($48 \pm 13\%$, $P < 0.01$). Consistently in both analyses, there is no difference between the two directions of the interactions ($12 \pm 7\%$, $P > 0.05$). In the movie–noise paradigm, we find that the decrease of the total interactions found in the trial-by-trial analysis is not reproduced in the ensemble analysis for the naïve animals (movie: $-12 \pm 14\%$; noise: $-10 \pm 13\%$; $P > 0.05$ in both cases, see Fig. 6B, left) as well as for the trained animals (movie: $31 \pm 18\%$; noise: $33 \pm 20\%$; $P > 0.05$ in both cases). But consistently between the two analyses, neither bottom-up nor top-down dominates in this paradigm in naïve (movie: $31 \pm 18\%$; noise: $12 \pm 15\%$; $P > 0.05$ in both cases, see also Fig. 6B, right) or in trained animals (movie: $17 \pm 12\%$; noise: $15 \pm 14\%$; $P > 0.05$ in both cases). Finally, in the grating paradigm, both types of analysis yield the same result for naïve animals, that is, no effect of the stimulus (total interaction: $70 \pm 41\%$; differential interaction: $15 \pm 17\%$, $P > 0.05$ in both cases). Altogether, the significance of some of the results depends on the type of analysis and, thus, on the initial assumption about the uniqueness of the process underlying interareal interactions. But other results were found consistently in the two analyses: the lack of relation between the differential interactions and the stimulus structure and, more importantly, the increase of the total interactions by S^+ and S^-.

We furthermore employ a different frequency analysis of the interactions, the so-called directed transfer function. This is computed from the MVAR models obtained using the ensemble analysis. For the grating–food paradigm we compute the frequency spectra of the differential interactions in a similar way to the results presented in Fig. 3B. In agreement with those results, the prominent difference between the two stimuli S^+ and S^- occurs in the gamma frequency range mainly between 30 and 70 Hz.

Discussion

In the present study, we measured local field potentials in alert cats and quantified the flow of information between primary visual cortex (A17/18) and area A21a. To determine the effects of stimulus structure and of expectancy on the modulation of interareal interactions, we analysed data from two different paradigms. In a first paradigm, natural movies and their derived pink noise stimuli decreased the total interareal interactions. This result, however, reached significance only in the trial-by-trial and not in the ensemble analysis; these analyses differ in their assumption about the uniqueness of the process underlying interareal interactions and this issue is discussed below. Nevertheless, there was no consistent dominance of either bottom-up or top-down interactions in this paradigm. In a second paradigm, during the presentation of stimuli associated with a possible delivery of food, the total interactions were found to increase in the two types of analysis. Furthermore, whether a 'reward' could be expected or not influenced the contribution of top-down and bottom-up signals to interareal interactions. This effect was maximal in proximity to the expected event and mostly expressed in the gamma range of the local field potential.

One issue about the causality measures used here is that the influence of a third area cannot be ruled out. In general, two variables X and Y could be driven by a third variable Z that is not measured. Assume that the coupling between Z and X has a shorter latency than the coupling of Z to Y. Then, applying the Wiener–Granger causality analysis to the pair (X, Y) would yield a directed interaction from Y to X. Therefore, common input to the two areas is not only reflected in the instantaneous interaction but can also affect bottom-up and top-down components. However, such common input should play only a minor role in the present case. First, the two areas of interest, A17/18 and A21a, are joined by direct connections both in bottom-up and in top-down directions (Stone *et al*., 1979; Rosenquist, 1985; Wang *et al*., 2000). Second, bottom-up connections from A17/18 provide a major excitatory drive to area A21a (Michalski *et al*., 1993) and top-down input from A21a modulates responses in A17 (Wang *et al*., 2000). Last, there are only few areas providing a major and direct common input: two areas 17/18 and 21a (see Burke *et al*. 1998 for an example). Areas 19 and posteromedial lateral suprasylvian area (PMLS) are possible candidates though. These points support the assumption that most of the interactions reported in this study are actually due to direct interactions between areas A17/18 and A21a and not due to common input.

A second issue is the common reference used for recording the local field potentials. The four local field potentials recorded simultaneously at the different recording sites were all amplified with respect to the same common reference. This introduces a signal common to all channels and might influence the interaction measures. One way to overcome this problem is to use bipolar electrodes where electrode and reference are closely spaced together (see von Stein *et al*., 2000 for an example). However, this approach requires a specifically designed electrode and amplification set up. Instead of performing such a local differentiation using the amplifier hardware, one could consider doing so offline. This requires that all channels have been recorded with exactly the same amplification gain factor. This gain, however, depends not only on the details of the amplifier set up but also on the electrode impedance. The latter could in principle be measured even after implantation, but is subject to uncontrollable and continuous changes, e.g. due to tissue reactions. Thus, offline differentiation could in principle be done, but the quality of the result is uncertain and it is practically impossible to determine what proportion of the signal is due to a common reference. We thus relied on the signals as they were recorded without adding a further step of uncertainty. Furthermore, a common signal originating from the same reference should mainly affect the instantaneous component of the interactions, a measure that was not included in the study (see Materials and methods).

A third issue requiring discussion is the different results obtained from the trial-by-trial and ensemble analyses. The fundamental difference between the two approaches is the assumption that, in the ensemble analysis, all the trials are the realizations of the same stochastic process and thus follow (up to small noise) the same multivariate model. Based on this assumption, the ensemble analysis combines the data from all trials to find the 'mean model' that fits the observed interactions. On the other hand, the trial-by-trial analysis allows a different model for each trial and describes the interaction based on these varying models. Both methods have their advantages and it is, *a priori*, not clear which method is more valid. If we assume that bottom-up and top-down signals strictly follow a fixed scheme that depends only on their level of involvement and thus on the experimental paradigm, the ensemble analysis would be a good

choice. However, it might well be that these interactions follow certain dynamics and, thus, are not stationary from trial to trial; as it is well documented for neuronal responses (Schiller *et al*., 1976; Vogels *et al*., 1989). In this case, the best approach is to describe interareal interactions by using different models in different trials, which can be achieved by the trial-by-trial analysis. In contrast, the ensemble analysis would yield less accurate, if not plainly misleading, results. For example, the behavioural relevance of a stimulus could influence the consistency of interareal interactions by reducing the trial-by-trial variability in the grating–food paradigm compared with the movie–noise paradigm. If this were the case, both types of analysis would yield similar results in the first but not in the latter paradigm, which is what we observed. To conclude, which method of analysis is adequate might well depend on multiple factors and, in general, needs further investigation. Nevertheless, the trial-by-trial analysis rests on fewer assumptions than the ensemble analysis. One consequence may be a weaker sensitivity to stimulus-induced interactions but, more importantly, it is less restrictive and its results have a more general validity.

The results from the trial-by-trial analysis show that the relative changes of interareal interactions decrease when viewing natural movies and their derived pink noise. This is an unexpected result because both realistic and noise stimuli were shown to induce strong activations of local field potentials within area A17/18 (Kayser *et al*., 2003) and similarly within area A21a (unpublished data). One possible explanation is that the complexity and, in the present experimental context, the unpredictability of movie and noise stimuli emphasizes local and intra-areal interactions at the detriment of interareal processing. Furthermore, these results do not support an important role of top-down signals in structuring and grouping information in lower areas of the visual system (Hupe *et al*., 1998; Lamme *et al*., 1998; Lamme & Roelfsema, 2000; Bullier *et al*., 2001). However, we cannot completely rule out this hypothesis for the following reasons. First, the interactions of trained cats are dominated by top-down signals, albeit only during the second half of the stimulus presentation. Second, the method used to quantify these interactions is based on an MVAR model of the local field potentials and thus is limited to a certain timescale that is determined by the order of the model and by the sampling rate of the data. Therefore, it is still possible that top-down signals carry information about perceptual grouping on a fast timescale (Hupe *et al*., 2001).

In contrast, simple gratings do not affect interactions between areas in naïve animals and lead to an imbalance of top-down and bottom-up components when presented in a context where food deliveries can be expected. Interestingly, this increase in interareal interactions occurs in a similar manner for both top-down and bottom-up directions between 200 and 1000 ms from stimulus onset. Whether food delivery can be expected or not changes the contribution of top-down and bottom-up signals in the later part of the response. As the differential interaction (top-down minus bottom-up) has a positive value when a reward is predictable, albeit not significantly different from zero, this result is in favour of a role for top-down signals in processing predictions (Rao & Ballard, 1997, 1999; Engel *et al*., 2001). Furthermore, the characterization of these discriminative signals in the gamma range is in accordance with previous reports (see Engel *et al*., 2001 for a review).

What are the internal processes modulating interactions when forthcoming events are predictable? Theoretically, motor planning could affect interactions between visual areas. However, this is unlikely in the present case because the animal was passively viewing the stimuli and no instrumental response was required. Indeed, the only obvious action expressed was the consumption of the food delivered after stimulus offset. Even if such an action was planned, it is inconceivable that this planning occurred more than 1 s in advance, the time at which differential interactions discriminate between stimuli. Thus, motor planning solely cannot account for the full extent of the modulations. Another possibility is that forthcoming events activate several mental processes such as predictions, expectations, attention and alertness. These processes interact and influence each other dynamically. For example, the food delivery can be predicted upon identification of the stimulus. Such a prediction could generate a state of expectancy and increase the general level of attention and alertness. Thus, these processes are very difficult to differentiate and this is not within the scope of the present study. As the key component of these processes is the generation of predictions, we emphasize this aspect.

The neuronal correlate of predictions, such as expected rewards, has been assessed both with firing rates (see Schultz, 2000 for a review) and spike synchronization (Vaadia *et al*., 1995; de Oliveira *et al*., 1997). Expectations are supposedly formed in the frontal cortex, but are also visible as changes of synchrony in other areas such as in the primary motor cortex (Riehle *et al*., 1997). This suggests that predictions spread through the cortex in a top-down manner. Our data are in agreement with this idea, and furthermore emphasize the cooperation between top-down and bottom-up signals in interareal interactions. Indeed, statistical significances were consistently found for the total interactions and not for the differential interactions. Furthermore, as gamma oscillations are considered as a good index of synchronous spiking (Fries *et al*., 1997; Gray & Viana Di Prisco, 1997; Herculano-Houzel *et al*., 1999; Gail *et al*., 2000; Maldonado *et al*., 2000), our results are compatible with a role of synchrony in encoding expectations.

Perceptual learning (Ahissar *et al*., 1992; Recanzone *et al*., 1992, 1993; Merzenich & Sameshima, 1993; Logothetis *et al*., 1995; Ahissar & Hochstein, 1997; Kobatake *et al*., 1998; Crist *et al*., 2001; Schoups *et al*., 2001; Hochstein & Ahissar, 2002; Lee *et al*., 2002) and visuomotor training (Salazar *et al*., 2004) have been associated with changes in sensory cortices. Common supervised learning schemes require that a reinforcement signal reaches the site of learning. Thus, there is a timing restriction for this signal if it has to induce changes in distant areas. At the level of synapses, plasticity operates within a temporal window of 10s of milliseconds (Gerstner *et al*., 1996; Markram *et al*., 1997). If the changes observed after perceptual learning and visuomotor training follow supervised learning schemes and are induced by synaptic plasticity, then sensory and reinforcement signals have to reach single neurons within this time range. One way to decrease the time delay between these signals is to anticipate future events in order to transmit the reinforcement signal in advance. To facilitate learning and synaptic plasticity, higher areas may generate expectations and predictions about future sensory events (Schultz, 1998; Waelti *et al*., 2001; Schultz, 2002; Fiorillo *et al*., 2003), which are transmitted to sensory areas in a top-down manner. Thereby, bottom-up information about the sensory stimulus and top-down predictions could operate on a timescale suitable for synaptic plasticity.

Acknowledgements

This work was funded by the Swiss National Science Foundation (grant nr: 31-65415.01) and by the Neuroscience Center Zürich. We thank Muir D. and Onat S. for comments on an earlier version of this manuscript, and the two referees for their constructive remarks.

Abbreviations

AIC, Akaike Information Criterion; MVAR, multivariate autoregressive; r.m.s., root mean square.

References

Ahissar, M. & Hochstein, S. (1997) Task difficulty and the specificity of perceptual learning. *Nature*, **387**, 401–406.

Ahissar, E., Vaadia, E., Ahissar, M., Bergman, H., Arieli, A. & Abeles, M. (1992) Dependence of cortical plasticity on correlated activity of single neurons and on behavioural context. *Science*, **257**, 1412–1415.

Akaike, H. (1974) A new look at the statistical model identification. *IEEE Trans. Autom Control*, **19**, 716–723.

Baccala, L.A. & Sameshima, K. (2001) Partial directed coherence: a new concept in neural structure determination. *Biol. Cybern.*, **84**, 463–474.

Bernasconi, C. & König, P. (1999) On the directionality of cortical interactions studied by structural analysis of electrophysiological recordings. *Biol. Cybern.*, **81**, 199–210.

Betsch, B.Y., Einhäuser, W., Körding, K.P. & König, P. (2004) The world from a cat's perspective – statistics of natural videos. *Biol. Cybern.*, **90**, 41–50.

Brainard, D.H. (1997) The psychophysics toolbox. *Spat. Vis.*, **10**, 433–436.

Bullier, J., Hupe, J.M., James, A.C. & Girard, P. (2001) The role of feedback connections in shaping the responses of visual cortical neurons. *Prog. Brain Res.*, **134**, 193–204.

Burke, W., Dreher, B. & Wang, C. (1998) Selective block of conduction in Y optic nerve fibres: significance for the concept of parallel processing. *Eur. J. Neurosci.*, **10**, 8–19.

Crist, R.E., Li, W. & Gilbert, C.D. (2001) Learning to see: experience and attention in primary visual cortex. *Nat. Neurosci.*, **4**, 519–525.

Ding, M., Bressler, S.L., Yang, W. & Liang, H. (2000) Short-window spectral analysis of cortical event-related potentials by adaptive multivariate autoregressive modeling: data preprocessing, model validation, and variability assessment. *Biol. Cybern.*, **83**, 35–45.

Engel, A.K., Fries, P. & Singer, W. (2001) Dynamic predictions: oscillations and synchrony in top-down processing. *Nat. Rev. Neurosci.*, **2**, 704–716.

Felleman, D.J. & Van Essen, D.C. (1991) Distributed hierarchical processing in the primate cerebral cortex. *Cereb. Cortex*, **1**, 1–47.

Fiorillo, C.D., Tobler, P.N. & Schultz, W. (2003) Discrete coding of reward probability and uncertainty by dopamine neurons. *Science*, **299**, 1898–1902.

Freiwald, W.A., Valdes, P., Bosch, J., Biscay, R., Jimenez, J.C., Rodriguez, L.M., Rodriguez, V., Kreiter, A.K. & Singer, W. (1999) Testing non-linearity and directedness of interactions between neural groups in the macaque inferotemporal cortex. *J. Neurosci. Meth.*, **94**, 105–119.

Fries, P., Roelfsema, P.R., Engel, A.K., König, P. & Singer, W. (1997) Synchronization of oscillatory responses in visual cortex correlates with perception in interocular rivalry. *Proc. Natl Acad. Sci. USA*, **94**, 12699–12704.

Gail, A., Brinksmeyer, H.J. & Eckhorn, R. (2000) Contour decouples gamma activity across texture representation in monkey striate cortex. *Cereb. Cortex*, **10**, 840–850.

Galuske, R.A., Schmidt, K.E., Goebel, R., Lomber, S.G. & Payne, B.R. (2002) The role of feedback in shaping neural representations in cat visual cortex. *Proc. Natl Acad. Sci. USA*, **99**, 17083–17088.

Gerstner, W., Kempter, R., van Hemmen, J.L. & Wagner, H. (1996) A neuronal learning rule for sub-millisecond temporal coding. *Nature*, **383**, 76–81.

Geweke, J. (1982) Measurement of conditional linear dependence and feedback between multiple time series. *J. Am. Stat. Assoc.*, **77**, 304–313.

Granger, C. (1963) Economic processes involving feedback. *Inf. Control*, **6**, 28–48.

Granger, C. (1969) Investigating causal relations by econometric models and cross-spectral methods. *Econometrica*, **37**, 424–438.

Granger, C. (1980) Testing for causality: a personal viewpoint. *J. Econ. Dyn. Control*, **2**, 329–352.

Gray, C.M. & Viana Di Prisco, G. (1997) Stimulus-dependent neuronal oscillations and local synchronization in striate cortex of the alert cat. *J. Neurosci.*, **17**, 3239–3253.

Haykin, S. & Kesler, S. (1983) Prediction error filtering and maximum entropy spectral estimation. In Haykin, S. (Ed.), *Non-Linear Methods of Spectral Analysis.* Springer, Berlin, pp. 9–72.

Herculano-Houzel, S., Munk, M.H., Neuenschwander, S. & Singer, W. (1999) Precisely synchronized oscillatory firing patterns require electroencephalographic activation. *J. Neurosci.*, **19**, 3992–4010.

Hochstein, S. & Ahissar, M. (2002) View from the top: hierarchies and reverse hierarchies in the visual system. *Neuron*, **36**, 791–804.

Hupe, J.M., James, A.C., Girard, P., Lomber, S.G., Payne, B.R. & Bullier, J. (2001) Feedback connections act on the early part of the responses in monkey visual cortex. *J. Neurophysiol.*, **85**, 134–145.

Hupe, J.M., James, A.C., Payne, B.R., Lomber, S.G., Girard, P. & Bullier, J. (1998) Cortical feedback improves discrimination between figure and background by V1, V2 and V3 neurons. *Nature*, **394**, 784–787.

Jenkins, G.M. & Watts, D.G. (1968) *Spectral Analysis and its Applications*. Holden-Day, San Francisco.

Kaminski, M., Ding, M., Truccolo, W.A. & Bressler, S.L. (2001) Evaluating causal relations in neural systems: Granger causality, directed transfer function and statistical assessment of significance. *Biol. Cybern.*, **85**, 145–157.

Kayser, C., Salazar, R.F. & König, P. (2003) Responses to natural scenes in cat V1. *J. Neurophysiol.*, **90**, 1910–1920.

Kobatake, E., Wang, G. & Tanaka, K. (1998) Effects of shape-discrimination training on the selectivity of inferotemporal cells in adult monkeys. *J. Neurophysiol.*, **80**, 324–330.

Lamme, V.A. & Roelfsema, P.R. (2000) The distinct modes of vision offered by feedforward and recurrent processing. *Trends Neurosci.*, **23**, 571–579.

Lamme, V.A., Super, H. & Spekreijse, H. (1998) Feedforward, horizontal, and feedback processing in the visual cortex. *Curr. Opin. Neurobiol.*, **8**, 529–535.

Lee, T.S., Yang, C.F., Romero, R.D. & Mumford, D. (2002) Neural activity in early visual cortex reflects behavioral experience and higher-order perceptual saliency. *Nat. Neurosci.*, **5**, 589–597.

Liang, H., Bressler, S.L., Ding, M., Truccolo, W.A. & Nakamura, R. (2002) Synchronized activity in prefrontal cortex during anticipation of visuomotor processing. *Neuroreport*, **13**, 2011–2015.

Liang, H., Ding, M., Nakamura, R. & Bressler, S.L. (2000) Causal influences in primate cerebral cortex during visual pattern discrimination. *Neuroreport*, **11**, 2875–2880.

Logothetis, N.K., Pauls, J. & Poggio, T. (1995) Shape representation in the inferior temporal cortex of monkeys. *Curr. Biol.*, **5**, 552–563.

Lomber, S.G., Cornwell, P., Sun, J.S., MacNeil, M.A. & Payne, B.R. (1994) Reversible inactivation of visual processing operations in middle suprasylvian cortex of the behaving cat. *Proc. Natl Acad. Sci. USA*, **91**, 2999–3003.

Maldonado, P.E., Friedman-Hill, S. & Gray, C.M. (2000) Dynamics of striate cortical activity in the alert macaque. II. Fast time scale synchronization. *Cereb. Cortex*, **10**, 1117–1131.

Markram, H., Lubke, J., Frotscher, M. & Sakmann, B. (1997) Regulation of synaptic efficacy by coincidence of postsynaptic APs and EPSPs. *Science*, **275**, 213–215.

Merzenich, M.M. & Sameshima, K. (1993) Cortical plasticity and memory. *Curr. Opin. Neurobiol.*, **3**, 187–196.

Michalski, A., Wimborne, B.M. & Henry, G.H. (1993) The effect of reversible cooling of cat's primary visual cortex on the responses of area 21a neurons. *J. Physiol. (Lond.)*, **466**, 133–156.

de Oliveira, S.C., Thiele, A. & Hoffmann, K.P. (1997) Synchronization of neuronal activity during stimulus expectation in a direction discrimination task. *J. Neurosci.*, **17**, 9248–9260.

Pelli, D.G. (1997) The VideoToolbox software for visual psychophysics: transforming numbers into movies. *Spat. Vis.*, **10**, 437–442.

Rao, R.P. & Ballard, D.H. (1997) Dynamic model of visual recognition predicts neural response properties in the visual cortex. *Neural Comput.*, **9**, 721–763.

Rao, R.P. & Ballard, D.H. (1999) Predictive coding in the visual cortex: a functional interpretation of some extra-classical receptive-field effects. *Nat. Neurosci.*, **21**, 79–87.

Recanzone, G.H., Merzenich, M.M., Jenkins, W.M., Grajski, K.A. & Dinse, H.R. (1992) Topographic reorganization of the hand representation in cortical area 3b owl monkeys trained in a frequency-discrimination task. *J. Neurophysiol.*, **67**, 1031–1056.

Recanzone, G.H., Schreiner, C.E. & Merzenich, M.M. (1993) Plasticity in the frequency representation of primary auditory cortex following discrimination training in adult owl monkeys. *J. Neurosci.*, **13**, 87–103.

Riehle, A., Grun, S., Diesmann, M. & Aertsen, A. (1997) Spike synchronization and rate modulation differentially involved in motor cortical function. *Science*, **278**, 1950–1953.

Roelfsema, P.R., Engel, A.K., König, P. & Singer, W. (1997) Visuomotor integration is associated with zero time-lag synchronization among cortical areas. *Nature*, **385**, 157–161.

Rosenquist, A.C. (1985) Connections of visual cortical areas in the cat. In Peters, A. & Jones, E.G. (Eds), *Cerebral Cortex*, Vol. 3. Visual Cortex. Plenum Press, New York, pp. 81–116.

Salazar, R.F., Kayser, C. & König, P. (2004) Effects of training on neuronal activity and interactions in primary and higher visual cortices in the alert cat. *J. Neurosci.*, **24**, 1627–1636.

Schiller, P.H., Finlay, B.L. & Volman, S.F. (1976) Short-term response variability of monkey striate neurons. *Brain Res.*, **105**, 347–349.

Schoups, A., Vogels, R., Qian, N. & Orban, G. (2001) Practising orientation identification improves orientation coding in V1 neurons. *Nature*, **412**, 549–553.
Schultz, W. (1998) Predictive reward signal of dopamine neurons. *J. Neurophysiol.*, **80**, 1–27.
Schultz, W. (2000) Multiple reward signals in the brain. *Nat. Rev. Neurosci.*, **1**, 199–207.
Schultz, W. (2002) Getting formal with dopamine and reward. *Neuron*, **36**, 241–263.
von Stein, A., Chiang, C. & König, P. (2000) Top-down processing mediated by interareal synchronization. *Proc. Natl Acad. Sci. USA*, **97**, 14748–14753.
Stone, J., Dreher, B. & Leventhal, A.G. (1979) Hierarchical and parallel mechanisms in the organization of visual cortex. *Brain Res. Rev.*, **1**, 345–394.
Vaadia, E., Haalman, I., Abeles, M., Bergman, H., Prut, Y., Slovin, H. & Aertsen, A. (1995) Dynamics of neuronal interactions in monkey cortex in relation to behavioural events. *Nature*, **373**, 515–518.
Van Essen, D.C., Anderson, C.H. & Felleman, D.J. (1992) Information processing in the primate visual system: an integrated systems perspective. *Science*, **255**, 419–423.
Vogels, R., Spileers, W. & Orban, G.A. (1989) The response variability of striate cortical neurons in the behaving monkey. *Exp. Brain Res.*, **77**, 432–439.
Waelti, P., Dickinson, A. & Schultz, W. (2001) Dopamine responses comply with basic assumptions of formal learning theory. *Nature*, **412**, 43–48.
Wang, C., Waleszczyk, W.J., Burke, W. & Dreher, B. (2000) Modulatory influence of feedback projections from area 21a on neuronal activities in striate cortex of the cat. *Cereb. Cortex*, **10**, 1217–1232.